

EFFECT OF INTERNAL FLOWS ON SUNYAEV-ZELDOVICH MEASUREMENTS OF CLUSTER PECULIAR VELOCITIES

DAISUKE NAGAI^{1,2}, ANDREY V. KRAVTSOV^{1,2}, ARTHUR KOSOWSKY^{1,3}
Draft version February 7, 2020

ABSTRACT

Galaxy clusters are potentially powerful probes of the large-scale velocity field in the Universe because their peculiar velocity can be estimated directly via the kinematic Sunyaev-Zeldovich effect. This distortion of the microwave background is given by a density-weighted average over the peculiar velocity field of the cluster gas and only weakly depends on distance. Using high-resolution cosmological simulations of an evolving cluster of galaxies, we evaluate how well the averaged gas velocity on different scales reflects the actual cluster peculiar velocity, and how well Sunyaev-Zeldovich measurements can determine the peculiar velocity. The internal bulk velocities in the cluster gas are comparable to the overall cluster peculiar velocity, so sizable systematic velocity errors are expected. In an ideal situation with a noiseless map, the velocity averaged over the pixels of the kinematic Sunyaev-Zeldovich map inside a circular aperture matched to the cluster virial region provides an unbiased estimate of a cluster's radial peculiar velocity with a dispersion of 50 to 100 km/s. We discuss the extent to which these systematic errors might be modelled or averaged, and the resulting limitations on using galaxy clusters as cosmological velocity tracers.

Subject headings: cosmology: theory – intergalactic medium – methods: numerical – galaxies: clusters: general – instabilities – turbulence – X-rays: galaxies: clusters

1. INTRODUCTION AND MOTIVATION

Accurate maps of the cosmic velocity field would provide powerful constraints on the formation of structure in the Universe. A velocity field can be compared directly with measured galaxy density field, testing whether the fundamental picture of gravitational collapse is correct (Branchini et al. 2001; da Costa et al. 1998; Doré et al. 2002), or with velocity fields predicted by cosmological models, providing useful constraints on cosmological parameters and an independent measurement of the bias parameter on a range of scales. Indeed, intensive theoretical effort in the last decade produced very accurate predictions of various properties of the velocity fields from the linear to the highly nonlinear regime (e.g., Jing & Boerner 1998; Freudling et al. 1999; Juszkiewicz et al. 1999; Colín et al. 2000). However, despite clear theoretical importance, velocity surveys have been overshadowed by recent redshift surveys because peculiar velocities are far more difficult to measure than redshifts. Existing velocity surveys are thus more prone to systematic errors than redshift surveys. The main difficulty in measuring peculiar velocity is, of course, obtaining the distance to an object, which is necessary if the peculiar velocity is obtained by subtracting the Hubble flow velocity from a measured redshift velocity. Since distance errors tend to increase with distance, the reliability of redshift-based peculiar velocity surveys inevitably degrades with distance, making cosmological tests on large scales difficult.

Several groups have proposed using clusters of galaxies as tracers of the cosmic velocity field (Haehnelt & Tegmark 1996; Lange et al. 1998; Kashlinsky & Atrio-Barandela 2000; Aghanim et al. 2001; Peel & Knox 2002).

The peculiar velocity of a cluster can be measured in a single step, independent of the cluster distance, via the kinematic Sunyaev-Zeldovich effect (SZE : Zeldovich & Syunaev 1969; Sunyaev & Zel'dovich 1980); for recent reviews see Birkinshaw (1999) and Carlstrom et al. (2002). The electrons of the hot ionized gas in clusters Compton-scatter passing microwave background photons, resulting in a frequency-dependent redistribution of the photon energies (the thermal SZ effect). A smaller but measurable blackbody distortion arises from the Doppler shift due to bulk motion of the electrons with respect to the rest frame of the CMB photons (the kinematic SZ effect, hereafter kSZ). In principle, these effects can be distinguished by their spectral signatures, and, with sufficiently high angular resolution observations, the kSZ signal can be distinguished from intrinsic microwave background temperature fluctuations because galaxy clusters subtend angular scales small compared to characteristic primordial fluctuations. First measurements of the kSZ signal in clusters have been reported (Holzapfel et al. 1997), and several studies of the systematic errors related to disentangling the kSZ signal from other microwave fluctuations have been performed (Haehnelt & Tegmark 1996; Aghanim et al. 2001; Diego et al. 2002).

If clusters were simple spherical objects with negligible internal structure and motions (as has been assumed in several previous papers investigating the effect), then measurements of the kinematic SZ effect would provide a relatively straightforward method for measuring the cluster peculiar velocity. However, we know from high-resolution X-ray observations (i.e., Markevitch et al. 2000; Vikhlinin et al. 2001; Sun & Murray 2002; Mazzotta et al. 2002) and

¹ Center for Cosmological Physics, University of Chicago, Chicago IL 60637

² Department of Astronomy and Astrophysics, University of Chicago, 5640 S. Ellis Ave, Chicago IL 60637

³ Department of Physics and Astronomy, Rutgers University, 136 Frelinghuysen Road, Piscataway, NJ 08854-8019

numerical simulations (i.e., Norman & Bryan 1999; Ricker & Sarazin 2001) that galaxy clusters are actually complex objects with significant internal flows driven by frequent mergers. The observed kinematic SZ signal, which measures the density-weighted peculiar velocity of gas, will thus be some average over the bulk velocity and the internal velocities, which raises the question of how accurately an observed SZ signal will reflect the actual peculiar velocity of the cluster. Potential systematic errors can arise both because the gas itself does not necessarily reflect the bulk velocity of the matter and because observations with any effective flux limit will necessarily be biased towards the high-velocity portions of the mass distribution.

In this paper we use high-resolution simulations of a galaxy cluster formed in a Λ CDM cosmological model to investigate the systematic errors that can arise in estimates of the cluster velocity via the kSZ effect. In §2, we describe the cluster simulation used in our analysis. §3 explains how to estimate the peculiar velocity from kSZ maps, including the effects of noise. §4 discusses definitions of peculiar velocity and analyzes the systematic errors in the kSZ estimate. We summarize our results and discuss related issues in the final section.

2. NUMERICAL SIMULATIONS

We analyze a high-resolution cluster simulation performed using the Adaptive Refinement Tree (ART) N -body+gasdynamics code (Kravtsov 1999; Kravtsov et al. 2002). ART is an Eulerian code designed to achieve high spatial resolution by adaptively refining regions of interest, such as high-density regions or regions of steep gradients in gas properties, and has good shock-capturing characteristics. The code can capture discontinuities in gas properties within $\sim 1 - 2$ grid cells without using artificial viscosity, which makes it well-suited for studying sharp features such as shock fronts and studying velocity fields. At the same time, adaptive refinement in space and (non-adaptive) refinement in mass (Klypin et al. 2001) allows us to reach the large dynamic range required for high-resolution self-consistent simulations of cluster evolution in a cosmological setting.

The effects of magnetic fields, gas cooling, stellar feedback, and thermal conduction are not included in these simulations. As we show below, the systematic errors in the measurements of the radial peculiar velocity of clusters from kSZ observations arise mainly from the proximity of merging sub-clumps and the internal turbulent motion of cluster gas induced by mergers. These dynamical processes are expected to be largely unaffected by the neglected physical processes. More importantly, properly assessing the effect of gas flows requires simulations of cluster formation in a realistic cosmological setting, taking into account non-spherical accretion of matter along filaments along with major and minor mergers which induce the internal gas motions. The simulation analyzed here follows formation of a galaxy cluster from CDM initial conditions and has both very high mass and spatial dynamic range to model accurately the small-scale dynamics of dark matter and gas.

Specifically, we analyze a simulation of a cluster of intermediate mass in a Λ CDM model with $\Omega_m = 1 - \Omega_\Lambda = 0.3$, $\Omega_b = 0.043$, $h = 0.7$ and $\sigma_8 = 0.9$, where the Hubble con-

stant is defined as $100h \text{ km s}^{-1} \text{ Mpc}^{-1}$, and σ_8 is the rms density fluctuation on $8h^{-1} \text{ Mpc}$ scales. The simulation used a base 128^3 uniform grid and 7 levels of mesh refinement in a computational box of $80h^{-1} \text{ Mpc}$ with a peak formal resolution of $5h^{-1} \text{ kpc}$ and mass resolution (particle mass) of $2.7 \times 10^8 h^{-1} M_\odot$. At $z = 0$, the cluster has virial mass of $M_{340} = 2.4 \times 10^{14} h^{-1} M_\odot$ and virial radius of $R_{340} = 1.26h^{-1} \text{ Mpc}$, where the subscripts indicate the cosmology-dependent virial overdensity with respect to the mean density of the Universe. This Λ CDM cluster simulation was recently used in the analysis of “cold fronts” in clusters (Nagai & Kravtsov 2002), and further numerical details of the cluster simulation can be found there.

3. PECULIAR VELOCITIES FROM THE KINEMATIC SZ EFFECT

Can we measure the radial peculiar velocity of clusters using the kSZ effect accurately enough to learn about cosmology? The possible sources of uncertainty are intrinsic CMB anisotropies, superposition of several clusters along line of sight, errors in separation of thermal and kinematic SZ effects, and complex velocity structure within the cluster. To address the latter issue, we first construct kSZ distortion maps from the high-resolution cluster simulation at different epochs and along three orthogonal directions. We then estimate radial peculiar velocities from these maps and compare the value to the radial peculiar velocity of a cluster defined by the smoothed dark matter distribution.

3.1. Simulated kSZ Maps

The kSZ effect arises due to Compton scattering of CMB photons by ionized gas in motion with respect to the rest frame of the CMB. The resulting induced temperature fluctuation is

$$-\frac{\Delta T}{T}(\vec{x}) = b(\vec{x}) \equiv \sigma_T \int dl n_e v_r, \quad (1)$$

where σ_T is the Thompson cross section, n_e is the electron number density, v_r is the velocity component along the line of sight (in units of the speed of light), the integration is along the line of sight, and \vec{x} represents directions on the (flat) sky. We generate kSZ maps of the simulated cluster from uniform density and velocity grids centered on the minimum of cluster potential by numerically integrating Eq. 1. The density and velocity grids, in turn, were constructed using interpolation from the original mesh refinement structure. We then model measurements at a given resolution by convolving the maps with a Gaussian beam profile $A_\sigma(r)$ of appropriate width. Throughout this paper, we will assume a FWHM beamwidth of 1 arcminute. While individual clusters will be observed with higher resolution than this, it is unlikely that large SZ cluster surveys useful for cosmology will obtain significantly higher resolution in the near future. Higher resolution would not significantly alter our conclusions since the dominant systematic effects are unrelated to whether fine-scale structure is resolved in the maps.

Figure 1 shows kSZ maps of the simulated cluster at two different cosmic times (corresponding to redshifts $z = 0.43$ and $z = 0$) in three orthogonal projections. The top panels show the raw kSZ maps of a simulated cluster, with the earlier time in the top row. The size of the region

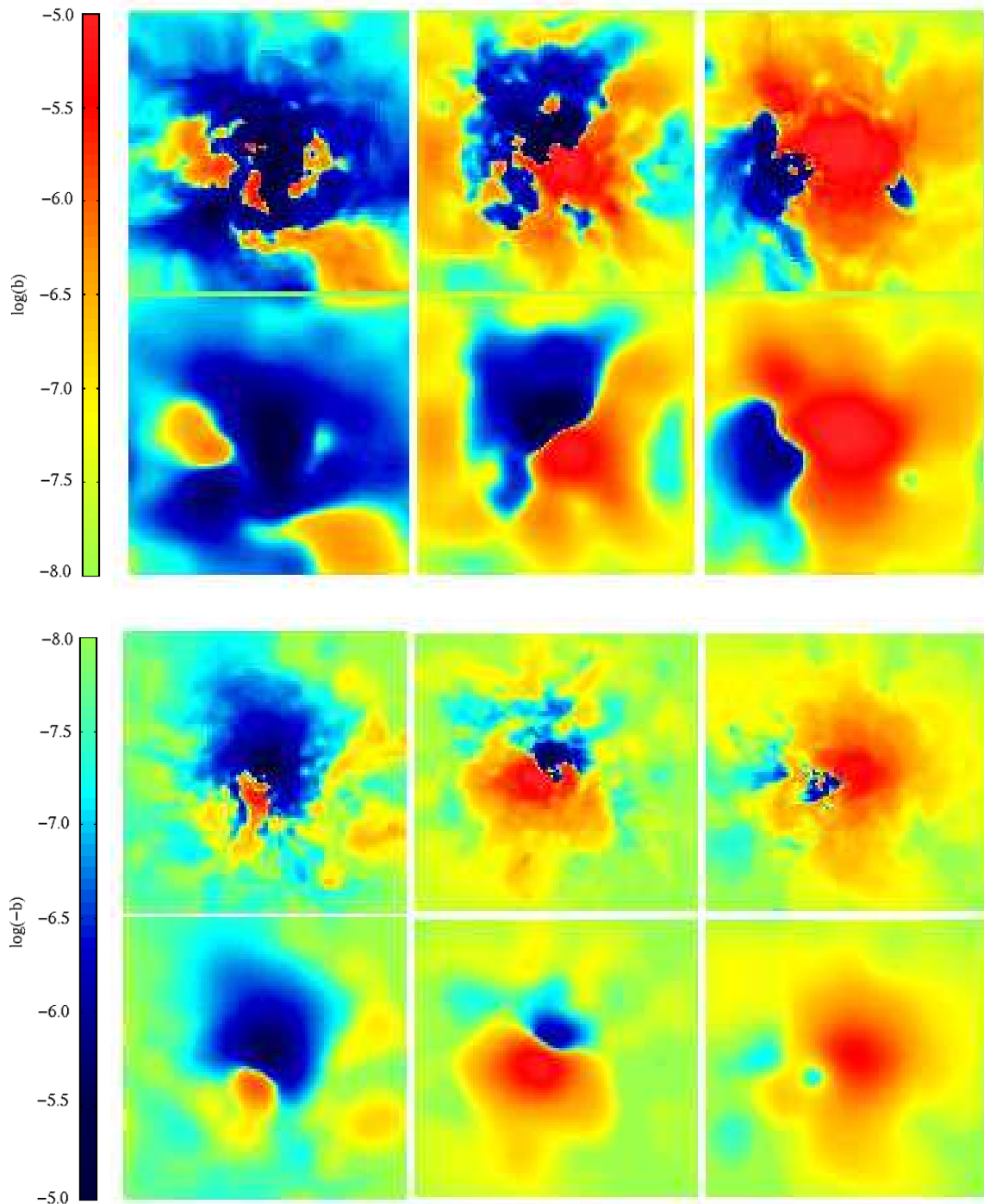


FIG. 1.— *First and third rows*: noiseless kinematic SZ Effect (kSZ) maps of the simulated Λ CDM cluster at redshifts $z = 0.43$ (1st row) and $z = 0$ (2nd row) through three orthogonal projections (from left to right). *Second and fourth rows*: the kSZ maps shown in the top panels convolved with a $1'$ (FWHM) Gaussian beam, assuming the cluster is at a distance corresponding to redshift $z = 0.1$. The maps are color-coded on a \log_{10} scale which is shown on the left hand side of the plots. The comoving size of the region shown is $2h^{-1}$ Mpc centered on the minimum of cluster potential, and the comoving pixel size is around $8h^{-1}$ kpc. Note that 1 arcminute corresponds to the physical scale $85 h^{-1}$ kpc at $z = 0.1$.

shown in the figure is $2h^{-1}$ comoving Mpc and the region is centered on the minimum of cluster potential. The comoving pixel size of the grid is $2h^{-1}$ Mpc/ $256 \approx 8h^{-1}$ kpc, close to the spatial resolution of the simulation. The bottom panels show the kSZ maps shown in the top panels convolved with a 1 arcminute FWHM Gaussian beam, as-

suming a cluster angular diameter distance corresponding to a redshift of $z = 0.1$. One arcminute corresponds to the physical scale $77.5h^{-1}$ kpc at $z = 0.1$ in the adopted Λ CDM cosmology. The smoothed maps are heavily over-sampled, with a pixel size around a tenth of the beam width. All maps are color-coded on a \log_{10} scale.

The high-resolution kSZ maps show a complex spatial structure of the kSZ distortion signal associated with internal motion of cluster gas and merging subclumps. At $z = 0.43$, the cluster is in a dynamically active stage; two nearly equal-mass sub-clusters have just undergone a slightly off-axis major merger and created strong merger shocks. In the top-left panel of Fig. 1, fast-moving gas ($\gtrsim 1000$ km/s) associated with the merger shock fronts appears as a large positive kSZ signal at the locations where the shock fronts are present, while the cluster as a whole is moving away from the observer, resulting in an overall negative kSZ signal when the raw kSZ signal is convolved with the Gaussian beam. In the top-middle panel of Fig. 1, the merger axis is aligned parallel to the line-of-sight direction, and the merger shock fronts propagating in both directions of the merger axis result in a dipole pattern in the kSZ signal. At $z = 0$, the cluster is in a relatively relaxed state, but continues to accrete matter and undergo minor mergers. In the bottom-middle panel, the merging subclump is moving parallel to the line of sight, appearing as the strongly negative kSZ signal (also note a small merging sub-clump to the left of the cluster center in Fig. 4). This behavior is generic for galaxy clusters in our simulations: even epochs where the cluster is “relaxed” minor merger(s) are typically present (see also Fig. 5). The ever-present internal motions within the cluster produce prominent substructure in the kSZ maps.

3.2. Velocity Estimates with a Noisy Map

How do we estimate the cluster peculiar velocity from an actual kSZ map? The most straightforward approach is to define some aperture centered on the cluster center (i.e., the peak of the thermal SZ signal or X-ray emission) and calculate the average velocity within the aperture. As we discuss below, if the map is noiseless, this *aperture average velocity* is, in fact, a largely unbiased estimator of a cluster’s radial peculiar velocity, and the error in each measurement will depend on the size and shape of the aperture used to select the cluster region for the analysis. For accurate velocity measurements, the aperture must be chosen large enough to encompass the bulk of the cluster region, and the optimal aperture is matched to the virial radius of the cluster.

Any actual kSZ map will be a sum of the true kSZ signal and noise, and the aperture average velocity will be composed of two terms: the signal average and the noise average. The noise arises from two main sources: instrumental noise and systematic errors from separating the kSZ signal from other microwave signals. For well-designed experiments, the instrumental noise should be close to Gaussian and largely uncorrelated between pixels. In this case, the noise average will be smaller than the pixel noise by a factor of $N^{1/2}$ for N pixels, and gives a random, Gaussian error contribution to any average velocity estimate. The rest of the noise is harder to characterize precisely and provide some irreducible noise floor for the observation. The separation of the kSZ signal from blackbody CMB fluctuations will induce some residual error, as will separation of foregrounds and thermal SZ signals; this noise does not have nice, well-understood properties and varies with the resolution, sensitivity, and frequency bands of an experiment.

One way to minimize the effect of the irreducible noise is to use a small aperture to exclude the noise-dominated region of the map from the analysis. More specifically, the size of the aperture might be limited to the inner region of the cluster with higher signal-to-noise, which typically corresponds to a half of the cluster virial radius or less. Alternatively, it is also possible to perform parametric source estimates such that the map regions with high signal-to-noise ratio provide the most constraint on the radial peculiar velocity estimate, with very little contributed by low signal-to-noise regions. While realistic projected sensitivities for upcoming SZ survey experiments are a few μK per square arcminute, we note that the effective flux limit is not determined simply by the instrumental noise in the map, but rather by irreducible systematic errors from component separation or other noise correlations. Below we will model the effect of noise with an effective flux limit and consider flux limits of 3 and 1 μK per map pixel. To mimic this situation, we estimate the *flux-limited average velocity* of the cluster by including only pixels with a kSZ flux larger than the flux limit. For any real experiment, averaging over a larger map region will give less biased estimates of the velocity and a smaller pixel noise average but potentially larger contributions from other systematic errors.

3.3. Estimating Radial Peculiar Velocity from kSZ Maps.

To construct a radial velocity estimator from the beam-smearred kSZ maps, we assume that all of the gas in the cluster is moving with a single radial bulk velocity, and then find this velocity from the maps. To examine the effect of aperture limit discussed above, we first define a circular aperture centered on the minimum of cluster potential and calculate the average velocity within the aperture. Below, we consider three different apertures relative to the cluster virial radius. To illustrate the effect of the flux limit, we calculate the average velocity using all pixels of the beam-convolved kSZ maps whose flux value is larger than the limit (no flux limit, 1 μK , and 3 μK). In both cases, we first calculate the beam-smearred kSZ flux $\langle b^B \rangle$ using all pixels selected according to each criterion. Using the same set of pixels, we then calculate the average beam-smearred electron column density $\langle \tau^B \rangle$. This is simple in the context of a simulation; see Sec. 5 for a discussion about estimating this quantity observationally. Then comparing with Eq. (1), the estimated radial velocity is simply

$$v_r^{\text{est}} = \frac{c}{\sigma_T} \frac{\langle b^B \rangle}{\langle \tau^B \rangle} \quad (2)$$

Note that, in the absence of a flux limit, the estimated radial peculiar velocity v_r^{est} is essentially equal to the aperture average velocity with an aperture matched to the virial radius of the cluster.

4. PECULIAR VELOCITIES

4.1. Definitions of Peculiar Velocity

To gauge the accuracy of estimated radial velocity from kSZ maps in the previous section, we need to define a reference “true” radial peculiar velocity. In the literature, the peculiar velocity is typically defined to be the density-weighted average dark matter velocity within a sphere of

some characteristic cluster radius. The most natural outer boundary of a cluster is given by the virial radius, but a fixed radius is also often used in the literature (e.g., Abell radius of 1.5 Mpc Bahcall et al. 1994; Croft & Efstathiou 1994; Colberg et al. 2000). We define v_r^{vir} as the density-weighted average dark matter velocity within the virial radius. In linear theory, the peculiar velocity is defined to be the velocity of a density peak of dark matter smoothed over $10h^{-1}\text{Mpc}$. In turn, the kSZ estimate of the radial peculiar velocity is the density-weighted average gas velocity well within the virial radius, as the kSZ signal is concentrated in the central region of the cluster.

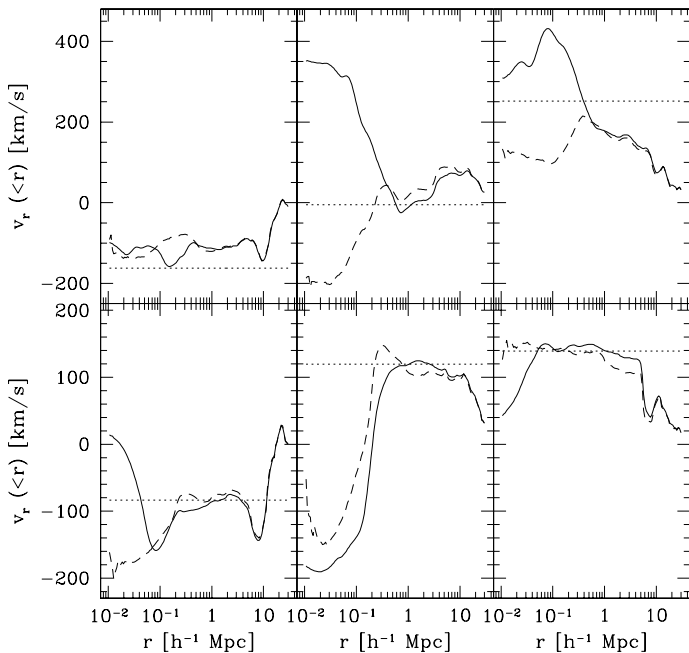


FIG. 2.— The density-weighted average radial velocities of gas (solid) and dark matter (dashed) within a sphere centered on the minimum of cluster potential for clusters at $z = 0.43$ (top) and $z = 0$ (bottom) through the same three orthogonal projections (from left to right) shown in Fig. 1. Dotted lines show the estimated radial velocity of a cluster v_r^{est} from kSZ observations; v_r^{est} is the average velocity within the aperture matched to the virial radius of the cluster. The density-weighted average velocities of gas and dark matter agree remarkably well beyond $\sim 500\text{kpc}$ (approximately half the cluster virial radius), particularly for the relaxed $z = 0$ cluster; however, the discrepancies are significant in the central region of the cluster.

To illustrate how various definitions of the peculiar velocity are related, we examine the density-weighted average gas and matter velocity profiles as a function of radius. Figure 2 shows the density-weighted average radial velocities of gas (solid) and dark matter (dashed) within a sphere centered on the minimum of the cluster potential at times corresponding to $z = 0.43$ (top) and $z = 0$ (bottom) through the same three orthogonal projections shown in Fig. 1. Dotted lines show the estimated radial velocity of a cluster v_r^{est} from kSZ observations; here, v_r^{est} is the average velocity within the aperture matched to the virial radius of the cluster.

The density-weighted average velocities of gas and dark matter agree remarkably well beyond $\sim 500\text{ kpc}$ (approximately half of the virial radius of the cluster); however,

the discrepancies are significant in the central region of the cluster. The discrepancy between the gas and dark matter velocity is most pronounced during the merger when the internal gas velocities exceed 1000 km/s . This is not surprising since dark matter and gas relax via different processes (gas through shocks and dark matter via violent relaxation). Note also that the peculiar velocity averaged within the virial radius can be significantly different from the velocity averaged over a larger scale (e.g., the difference with average velocity on $10h^{-1}\text{ Mpc}$ scales reaches $\gtrsim 50\%$ in some cases). The profiles show that, contrary to common assumption, clusters do not move as solid bodies and the choice of a peculiar velocity definition is somewhat arbitrary.

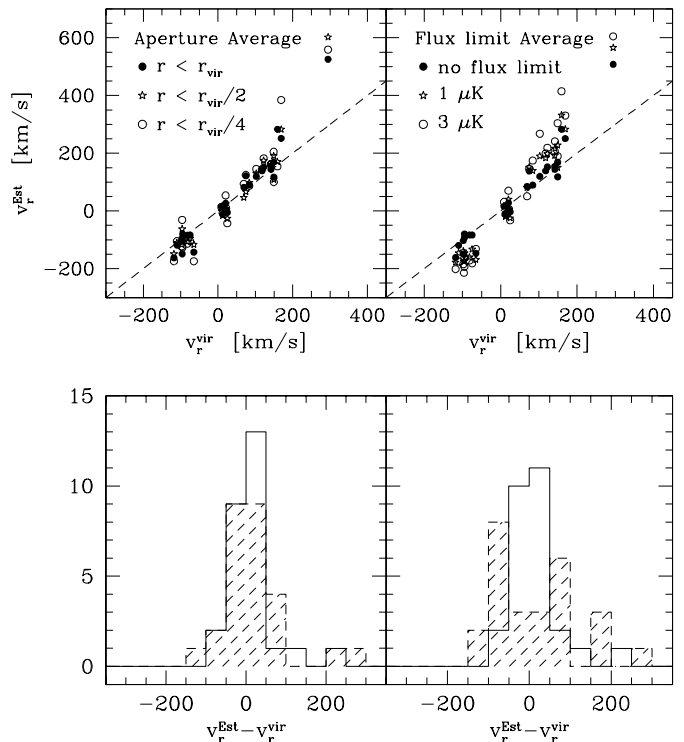


FIG. 3.— *Top* : the estimated radial velocities of a cluster from kSZ observations, v_r^{est} (Eq. (2)), are compared with the density-weighted average velocity of dark matter within the virial radius of the cluster, v_r^{vir} . We use cluster outputs at nine different redshifts ranging between 0.66 and 0.00 separated by intervals of a cluster dynamical time ($\sim 0.8\text{ Gyr}$) and evaluate v_r^{est} and v_r^{vir} for three orthogonal projections. In the left panel, v_r^{est} is the average velocity within an aperture matched to the virial radius r_{vir} (solid), $r_{\text{vir}}/2$ (star) and $r_{\text{vir}}/4$ (circle) of the cluster. In the right panel, we calculate v_r^{est} with no flux limit (solid) and flux limits of $1\text{ }\mu\text{K}$ (star) and $3\text{ }\mu\text{K}$ (circle). *Bottom* : a histogram of $v_r^{\text{est}} - v_r^{\text{vir}}$ for an aperture size matched to the virial radius r_{vir} (left : solid) and $r_{\text{vir}}/4$ (left : dotted-hatched), and the histogram for no flux limit (right : solid) and a flux limit of $3\text{ }\mu\text{K}$ (right : dotted-hatched). The aperture average radial velocity of a cluster from kSZ observations v_r^{est} is unbiased with a small dispersion of $\lesssim 50\text{ km s}^{-1}$; the flux-limited radial velocity is biased at a level of $50\text{-}100\text{ km s}^{-1}$.

4.2. The Accuracy of kSZ Peculiar Velocity Estimates

The top panel of Fig. 3 shows a comparison of the estimated radial velocities of a cluster from kSZ observations v_r^{est} and the density-weighted average velocity of dark matter within the virial radius of the cluster v_r^{vir} . We examine the simulated cluster at nine different redshifts ranging

between 0.66 and 0.00, with an interval of ~ 0.8 Gyr between redshifts, and evaluate v_r^{est} and v_r^{vir} for three orthogonal projections. The time interval is roughly equal to the dynamical time of the cluster, so the various epochs provide largely independent cluster configurations. In the left panel, v_r^{est} is the aperture average velocity within an aperture matched to the virial radius r_{vir} (solid), $r_{\text{vir}}/2$ (star) and $r_{\text{vir}}/4$ (circle) of the cluster. In the right panel, we calculate v_r^{est} with no flux limit (solid) and flux limits of $1 \mu\text{K}$ (star) and $3 \mu\text{K}$ (circle). The bottom-left panel of Fig. 3 shows a histogram of $v_r^{\text{est}} - v_r^{\text{vir}}$ for an aperture size matched to the virial radius r_{vir} (solid) and $r_{\text{vir}}/4$ (dotted-hatched). The bottom-right panel shows the histogram for no flux limit (solid) and a flux limit of $3 \mu\text{K}$ (dotted-hatched).

In the ideal situation where the map is noiseless, we find that the *aperture average velocity* is indeed an unbiased estimator of a radial peculiar velocity of the cluster. When the aperture encompasses the entire cluster virial region, the estimated velocity v_r^{est} agrees quite well with the true peculiar velocity of a cluster v_r^{vir} (top-left panel) with a small dispersion of $\lesssim 50 \text{ km s}^{-1}$ (bottom-left panel). When a smaller aperture is used to select the inner region of the cluster for the analysis, the estimated velocity is still unbiased, but the errors become larger; the error is $\simeq 100 \text{ km s}^{-1}$ if the aperture encompasses a region inside the quarter of the virial radius. The error in each measurement will depend not only on the size but also the shape of the aperture used to select the cluster region for the analysis. We consider a circular aperture for simplicity, but more elaborate apertures can be used. However, any aperture that puts more weight on the inner region of the cluster will likely lead to larger errors due to the internal bulk motions of gas at a level of $\sim 200 \text{ km s}^{-1}$ present in the central region of the cluster (see Fig. 2 and Fig. 4).

In addition, we find that a flux limit (i.e., averaging only over regions with fluxes above the limit) introduces a systematic bias in the estimated radial peculiar velocity. While the estimated radial peculiar velocity is unbiased in the absence of a flux limit, the magnitude of v_r^{est} is systematically overestimated; the bias grows with the flux limit. The bimodal distribution shown in the right panel of Fig. 3 also indicates the bias is indeed caused by the flux limit. Note that the magnitude of the radial peculiar velocity measurements will generally be overestimated, because the flux limit preferentially excludes regions whose bulk velocity is in the opposite direction from the cluster peculiar velocity, while keeping regions with bulk velocities in the same direction. Although the bias in the estimated velocity becomes substantial for effective flux limits as small as $0.3 \mu\text{K}$ per square arcminute, the correlation between the kSZ and virial velocity estimates is remarkably tight at any flux limit. This means that it may be possible to correct the systematic bias by using cluster simulations to model the kSZ signal in particular experiments.

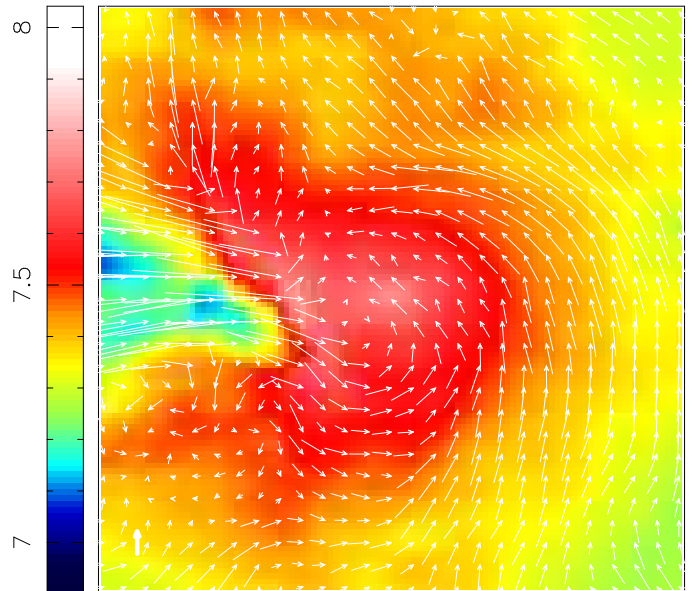


FIG. 4.— A gas velocity map overlaid on the emission-weighted temperature map of the cluster at $z = 0$ (projection corresponding to the left panel in Fig. 1). The gas velocity is the average projected velocity in a $78h^{-1}\text{Mpc}$ slice centered on the central density peak. The comoving size of the region is $0.82h^{-1}\text{Mpc}$. The length of the thick vertical vector in the bottom-left corner corresponds to 300 km s^{-1} ; the temperature maps are color-coded on a \log_{10} scale in units of degrees Kelvin.

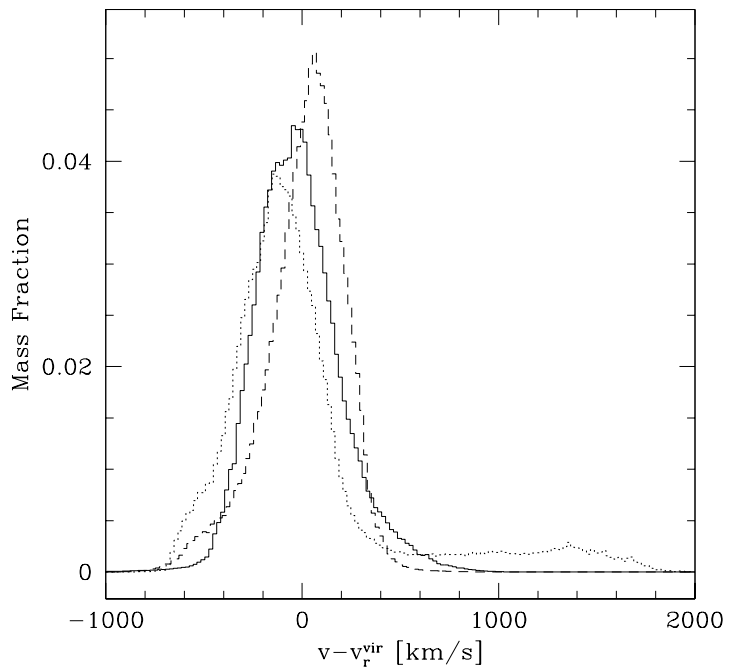


FIG. 5.— The distribution of the gas velocity component along three orthogonal projections (solid, dotted, and dashed correspond to the left, middle, and right panel projections in Fig. 1) within the virial radius of the cluster at $z = 0$.

To illustrate the structure and magnitude of internal flows, Figure 4 shows the velocity maps of gas overlaid on the emission-weighted temperature map of a cluster at $z = 0$ (projection corresponding to the left panel in Fig. 1). The velocity map shows the average gas velocity in a $78h^{-1} \text{ kpc}$ slice centered on the central density peak.

The comoving size of the displayed region is $0.82h^{-1}$ Mpc. The velocity map shows internal bulk motions of gas at a level of $\sim 200 \text{ km s}^{-1}$ within this relaxed cluster. The typical flow velocities are $\sim 10 - 30\%$ of the gas Mach number in the cluster core. Gas motions of a similar magnitude in the cores of relaxed clusters are also implied by the Chandra observations (Markevitch et al. 2002). Note also the merging sub-clump with velocity $\gtrsim 1000 \text{ km s}^{-1}$ on the left side of the main cluster. These prominent internal motions are essentially the cause of the bias in the peculiar velocity estimate: higher flux limits remove more of the quiescent gas and place more weight on the high-velocity regions, but this is precisely where the gas is least reliable at tracing the velocity as shown in Fig. 2. Regions of fast-moving gas are generally present even in “relaxed” clusters due to ongoing minor mergers.

The kSZ velocity estimates with no flux limit are in good agreement with v_r^{vir} for the cluster, with virial radii of $1.14h^{-1}$ Mpc for $z = 0.43$ and $1.26h^{-1}$ Mpc for $z = 0$; the agreement is particularly good at the lower redshift where the cluster is essentially relaxed. This means that the various large gas velocities average to the mean cluster velocity in general. Figure 5 shows the distribution of the gas velocity component along three orthogonal projections within the virial radius of the cluster at $z = 0$. The velocity distributions are Gaussian with velocity dispersion of $\sim 200 \text{ km s}^{-1}$, except for one case where a merging subclump has a line-of-sight velocity $\gtrsim 1000 \text{ km s}^{-1}$ (see also Fig. 4). The symmetric nature of the velocity distribution shows that the complete kSZ velocity estimate (without flux limit) will indeed reflect the true peculiar velocity, but that merging high-velocity substructures along the line of sight will bias even idealized no-flux-limit measurements. Our simulation suggests that such substructure occurs in a non-negligible fraction of clusters. Comparison of high-resolution kSZ maps and X-ray maps may identify such substructure on a case-by-case basis; the extent to which the effect of subclumps can be modelled from simulations remains to be seen. Without modelling, systematic errors on the order of 50 to 100 km/s in kSZ velocity estimates will occur in some fair number of clusters, although statistically these errors should be unbiased since we are as likely to observe subclumps falling in from either side of a cluster. Maps of the kSZ effect with 1 arcminute resolution should clearly identify the clusters with potentially serious errors from subclumps.

5. DISCUSSION AND CONCLUSIONS

Using a high-resolution N-body+gasdynamic cluster simulation in a Λ CDM cosmology, we have shown that

- i Arcminute-scale kSZ measurements will provide a generally accurate (with typical errors of $\lesssim 100 \text{ km/s}$) tracer of cluster peculiar velocities on scales of the cluster virial radius, but show significant discrepancies on scales smaller than half of the virial radius.
- ii In an ideal situation with a noiseless map, the velocity averaged over the kSZ map pixels inside a circular aperture matched to the cluster virial region provides an unbiased estimate a cluster’s radial peculiar velocity with a small dispersion of $\lesssim 50 \text{ km s}^{-1}$. When analyzing an actual kSZ map with noise, one may want

to use a smaller aperture to include only the region of the map with higher signal-to-noise; in such case, the velocity measurement is still unbiased, but with larger errors.

- iii Alternatively, flux-limited kSZ measurements with an effective flux limit as small as $3 \mu\text{K}$ per square arcminute can give significantly biased cluster peculiar velocity measurements (on order 100 km/s), and the bias increases with the flux limit. The measurements are essentially unbiased only if the flux limit is pushed below $0.1 \mu\text{K}$. However, biased flux-limited kSZ velocity estimates still have a fairly tight correlation with the density-weighted average dark matter velocity, so the bias can probably be accurately modelled for any given experiment.
- iv While accurate cluster velocity estimates might be obtained in a statistical sense from kSZ estimates, any individual cluster can give a significant velocity error due to random subclumps with velocities along the line of sight. Comparisons of high-resolution kSZ and X-ray maps can identify such subclumps, although it is unclear how accurately their effect can be modelled on a case-by-case basis.

Our estimated error amplitude agrees with the conclusions of Holder (2002). Although our analysis shows that the accurate measurements of radial peculiar velocity of clusters are possible, careful observational and theoretical studies of potential biases are required before we can use the kSZ peculiar velocity measurements to extract cosmological information.

Observationally, one needs thermal SZ effect and cluster gas temperature measurements to determine the beam-smearred column density, $\langle \tau^B \rangle = (m_e c^2 / \sigma_T k_B) \times [\langle y^B \rangle / \langle T_e \rangle_{n_e}^B]$, which enters Eq. 2. However, the density-weighted electron temperature $\langle T_e \rangle_{n_e}^B$ is not an observable; instead, the emission-weighted temperature of cluster gas $\langle T_X \rangle$ from the X-ray spectroscopy is often used. If the intracluster medium is isothermal throughout, then $\langle T_e \rangle_{n_e}^B = \langle T_X \rangle$. However, the non-isothermality of the intracluster medium revealed by recent high-resolution X-ray cluster observations (Markevitch et al. 1998; Peterson et al. 2001; Tamura et al. 2001; De Grandi & Molendi 2002) could introduce an additional bias in the kSZ measurements of the cluster peculiar velocity. Using rather low-resolution cluster simulations, Yoshikawa et al. (1998) reported that the use of $\langle T_X \rangle$ results in a systematic bias at a level of 5-15%. A better assessment of this effect requires high-resolution cluster simulations incorporating gas cooling and perhaps heating, physical processes which are likely important for the temperature structure in a cluster’s central region.

The Sunyaev-Zeldovich effect is independent of redshift and unable to distinguish between objects at different redshifts along the same line of sight. While the chance of two massive galaxy clusters being aligned is negligible (Voit et al. 2001), the probability for random alignment of a galaxy group ($M \simeq 10^{13}$ to $10^{14} M_\odot$) with a cluster will be somewhat higher and will appear like additional substructure in the kSZ map. If the group has a large line-of-sight velocity with the same sign as the cluster peculiar

velocity, it will be detectable in the same way as a high-velocity merging subclump, and might be modelled out in the same way. Groups with smaller peculiar velocities will bias the velocity determination and be harder to pick out in the kSZ maps. This systematic error will be small, considering that the high-velocity merging subclump in our simulation biases the velocity determination by around 50 km/s and a random galaxy will give a substantially smaller signal. This estimate is consistent with an assessment of this effect by Aghanim et al. (2001) who argue that random superposition of clusters with other objects along the line of sight leads to typical *rms* velocity errors of $\lesssim 100$ km/s. A more accurate estimation of this bias requires modelling with large-volume simulations.

We mention in passing that significant internal bulk velocities with characteristic amplitudes of 100 to 300 km/sec will greatly complicate measurements of cluster rotations with characteristic kSZ signals at the μK level, as proposed by Cooray & Chen (2002). A realistic assessment of this effect would need to use high-resolution simulated clusters, such as the one studied here.

Measuring blackbody kSZ distortions at the few μK level of course requires overcoming other systematics unrelated to the kSZ signal itself. Most importantly, galaxy clusters will possess a dominant thermal Sunyaev-Zeldovich distortion much larger than the kSZ signal. This thermal signal can, to some extent, be extracted via its departure from a blackbody spectrum using multiple frequency measurements, but relativistic corrections (Rephaeli 1995; Itoh et al. 2001) or departures from kinetic equilibrium (Blasi et al. 2000) can complicate this analysis (see Holder 2002). Second, the blackbody kSZ distortion must be separated from the blackbody primary temperature fluctuations of the microwave background. This can be accomplished via spatial filtering, since the primary microwave background fluctuations possess little power on cluster scales. The errors in filtering will give some unavoidable systematic error. Detailed simulations of the filtering process were done by Haehnelt & Tegmark (1996) and updated for currently envisioned experimental capabilities by Holder (2002). Aghanim et al. (2001) apply a simple filter to simulated Planck satellite maps, finding velocity errors due to the filtering of 300 to 600 km/s due to Planck's angular resolution. Upcoming ground-based experiments are likely to have higher sensitivity and reso-

lution than Planck, although with complications from atmospheric emission. The extent to which the kSZ signal can be isolated from the background fluctuations in arcminute resolution maps at high sensitivity needs to be studied in more detail. We anticipate systematic errors comparable to those from internal motions. Galactic dust emission and radio point sources are unlikely to be major problems at 200 GHz frequencies and arcminute angular scales, but lensed images of distant dusty galaxies could contribute a significant confusion noise (Blain 1998) and may need to be imaged at higher frequencies to extract the kSZ signal accurately.

Our simulated galaxy cluster shows that, perhaps contrary to naive expectation, the internal bulk flows in galaxy clusters do not present an insurmountable source of systematic error for peculiar velocity estimates based on the kinematic Sunyaev-Zeldovich effect. Aperture-averaged velocity estimates are largely unbiased. Effective flux limits will bias the velocity estimates towards higher values, but this effect does not induce a large dispersion in the velocity estimates and likely can be modelled with fair accuracy. High-velocity subclumps merging with the cluster along the line of sight will also induce systematic errors, but many of these clumps can be identified as particularly bright kSZ signals, and can be removed via comparison with X-ray maps. It is not unreasonable to hope that SZ cluster surveys will eventually produce cluster peculiar velocity catalogs with systematic velocity errors at a level of 50 km/s independent of the cluster distance. Velocity catalogs of such accuracy would provide a powerful probe of the growth of structure in the mildly nonlinear regime.

We would like to thank Lloyd Knox for useful discussion and comments, and Roman Juszkiewicz for asking questions prompting this study. The work presented here was partially supported by NASA through a Hubble Fellowship grant from the Space Telescope Science Institute, which is operated by the Association of Universities for Research in Astronomy, Inc., under NASA contract NAS5-26555 and by NSF through funding of the Center for Cosmological Physics at the University of Chicago (NSF PHY-0114422). DN thanks John Carlstrom for his support through NASA LTSA grant NAG5-7986. AK is a Cotrell Scholar of the Research Corporation.

REFERENCES

- Aghanim, N., Górski, K. M., & Puget, J.-L. 2001, *A&A*, 374, 1
 Bahcall, N. A., Gramann, M., & Cen, R. 1994, *ApJ*, 436, 23
 Birkinshaw, M. 1999, *Phys. Rep.*, 310, 97
 Blain, A. W. 1998, *MNRAS*, 297, 502
 Blasi, P., Olinto, A. V., & Stebbins, A. 2000, *ApJ*, 535, L71
 Branchini, E., Freudling, W., Da Costa, L. N., Frenk, C. S., Giovanelli, R., Haynes, M. P., Salzer, J. J., Wegner, G., & Zehavi, I. 2001, *MNRAS*, 326, 1191
 Carlstrom, J. E., Holder, G. P., & Reese, E. D. 2002, *ARA&A*, 40, 643
 Colin, P., Klypin, A. A., & Kravtsov, A. V. 2000, *ApJ*, 539, 561
 Colberg, J. M., White, S. D. M., Yoshida, N., MacFarland, T. J., Jenkins, A., Frenk, C. S., Pearce, F. R., Evrard, A. E., Couchman, H. M. P., Efstathiou, G., Peacock, J. A., Thomas, P. A., & The Virgo Consortium. 2000, *MNRAS*, 319, 209
 Cooray, A. & Chen, X. 2002, *ApJ*, 573, 43
 Croft, R. A. C. & Efstathiou, G. 1994, *MNRAS*, 268, L23
 da Costa, L. N., Nusser, A., Freudling, W., Giovanelli, R., Haynes, M. P., Salzer, J. J., & Wegner, G. 1998, *MNRAS*, 299, 425
 De Grandi, S. & Molendi, S. 2002, *ApJ*, 567, 163
 Diego, J., Hansen, S., & Silk, J. 2002, *MNRAS*, submitted (astro-ph/0207178)
 Doré, O., Knox, L., & Peel, A. 2002, *ApJ*, submitted (astro-ph/0207369)
 Freudling, W., Zehavi, I., da Costa, L. N., Dekel, A., Eldar, A., Giovanelli, R., Haynes, M. P., Salzer, J. J., Wegner, G., & Zaroubi, S. 1999, *ApJ*, 523, 1
 Haehnelt, M. G. & Tegmark, M. 1996, *MNRAS*, 279, 545
 Holder, G. P. 2002, *ApJ*, To be submitted (astro-ph/0207600)
 Holzapfel, W. L., Arnaud, M., Ade, P. A. R., Church, S. E., Fischer, M. L., Mauskopf, P. D., Rephaeli, Y., Wilbanks, T. M., & Lange, A. E. 1997, *ApJ*, 480, 449
 Itoh, N., Kawana, Y., Nozawa, S., & Kohyama, Y. 2001, *MNRAS*, 327, 567
 Jing, Y. P. & Boerner, G. 1998, *ApJ*, 503, 502
 Juszkiewicz, R., Springel, V., & Durrer, R. 1999, *ApJ*, 518, L25
 Kashlinsky, A. & Atrio-Barandela, F. 2000, *ApJ*, 536, L67
 Klypin, A., Kravtsov, A. V., Bullock, J. S., & Primack, J. R. 2001, *ApJ*, 554, 903
 Kravtsov, A. V. 1999, Ph.D. Thesis

- Kravtsov, A. V., Klypin, A., & Hoffman, Y. 2002, *ApJ*, 571, 563
- Lange, A. E., Church, S. E., & Holzapfel, W. 1998, *American Astronomical Society Meeting*, 30, 908
- Markevitch, M., Forman, W. R., Sarazin, C. L., & Vikhlinin, A. 1998, *ApJ*, 503, 77
- Markevitch, M., Ponman, T. J., Nulsen, P. E. J., Bautz, M. W., Burke, D. J., David, L. P., Davis, D., Donnelly, R. H., Forman, W. R., Jones, C., Kaastra, J., Kellogg, E., Kim, D. ., Kolodziejczak, J., Mazzotta, P., Pagliaro, A., Patel, S., Van Speybroeck, L., Vikhlinin, A., Vrtilik, J., Wise, M., & Zhao, P. 2000, *ApJ*, 541, 542
- Markevitch, M., Vikhlinin, A., & Forman, W. R. 2002, To appear in *ASP Conference Series*, (astro-ph/0208208)
- Mazzotta, P., Fusco-Femiano, R., & Vikhlinin, A. 2002, *ApJ*, 569, L31
- Nagai, D. & Kravtsov, A. V. 2002, *ApJ*, submitted (astro-ph/0206469)
- Norman, M. L. & Bryan, G. L. 1999, in *The radio galaxy Messier 87 : proceedings of a workshop held at Ringberg Castle, Tegernsee, Germany, 15-19 September 1997 / Hermann-Josef Röser, Klaus Meisenheimer, eds. Berlin ; New York : Springer, 1999. (Lecture notes in physics, 530, ISSN0075-8450).*, p.106, 106
- Peel, A. & Knox, L. 2002, To appear in *Proceedings of Dark Matter 2002*, (astro-ph/0205438)
- Peterson, J. R., Paerels, F. B. S., Kaastra, J. S., Arnaud, M., Reiprich, T. H., Fabian, A. C., Mushotzky, R. F., Jernigan, J. G., & Sakelliou, I. 2001, *A&A*, 365, L104
- Rephaeli, Y. 1995, *ApJ*, 445, 33
- Ricker, P. M. & Sarazin, C. L. 2001, *ApJ*, 561, 621
- Sun, M. & Murray, S. S. 2002, To appear in *ApJ*, Vol 576, 2002, (astro-ph/0206255)
- Sunyaev, R. A. & Zel'dovich, Y. B. 1980, *ARA&A*, 18, 537
- Tamura, T., Kaastra, J. S., Peterson, J. R., Paerels, F. B. S., Mittaz, J. P. D., Trudolyubov, S. P., Stewart, G., Fabian, A. C., Mushotzky, R. F., Lumb, D. H., & Ikebe, Y. 2001, *A&A*, 365, L87
- Vikhlinin, A., Markevitch, M., & Murray, S. S. 2001, *ApJ*, 551, 160
- Voit, G. M., Evrard, A. E., & Bryan, G. L. 2001, *ApJ*, 548, L123
- Yoshikawa, K., Itoh, M., & Suto, Y. 1998, *PASJ*, 50, 203
- Zeldovich, Y. B. & Syunayev, R. A. 1969, *Ap&SS*, 4, 301